

## Cable-pulley brace to improve story drift distribution of MRFs with large openings

Seyed Mehdi Zahrai and Seyed Amin Mousavi \*

*School of Civil Engineering, College of Engineering, the University of Tehran, Tehran, Iran*

*(Received January 19, 2016, Revised June 19, 2016, Accepted June 20, 2016)*

**Abstract.** This study aims to introduce a new bracing system by which even super-wide frames with large openings can be braced. The proposed system, hereafter called Cable-Pulley Brace (CPB), is a tension-only bracing system with a rectilinear configuration. In CPB, a wire rope passes through a rectilinear path around the opening(s) and connects the lower corner of the frame to its opposite upper one. CPB is a secondary load resisting system with a nonlinear-elastic hysteretic behavior due to its initial pre-tension load. As a result, the required energy dissipation would be provided by the MRF itself, and the main intention of using CPB is to contribute to the initial and post-yield stiffness of the whole system. Using a stiffness calibration technique, optimum placement of the CPBs is discussed to yield a uniform displacement demand along the height of the structure. A displacement-based design procedure is proposed by which the MRF with CPB can be designed to achieve a uniform distribution of inter-story drifts with predefined values. Obtained results indicated that CPB leads to significant reductions in maximum and residual deformations of the MRF at the expense of minor increase in the maximum base shear and developed axial force demands in the columns. In the case of a typical 5-story residential building, compared to SMRF system, CPB system reduces maximum amounts of inter-story and residual drifts by 35% and 70%, respectively. Moreover, openings of the frame are not interrupted by the CPB. This is the most appealing feature of the proposed bracing system from architectural point of view.

**Keywords:** wire rope; tension-only brace; cable brace; self-centering; residual drift; optimal stiffness distribution

### 1. Introduction

Modern architecture tends to widen frames with lots of windows to adjust itself with the current lifestyle. For such architectural designs, moment resisting frame (MRF) is the best alternative among other lateral load resisting systems. It is well understood that MRFs not only can be drift sensitive but also are prone to experience large residual deformations after a strong seismic event. Moreover, hysteretic behavior of a typical MRF is highly sensitive to its beam-to-column connections and strength deterioration can be triggered in the case of connections with poor seismic details. While some seismic codes have recognized importance of the residual deformations (ASCE 7 2010), they have provided no explicit provision about its allowable value. Excessive residual deformations not only would damage post-earthquake serviceability of the

---

\*Corresponding author, Ph.D. Candidate, E-mail: [s.a.mousavi@ut.ac.ir](mailto:s.a.mousavi@ut.ac.ir)

building, but also can amplify the  $P-\Delta$  effect during the subsequent aftershocks. There are very limited published studies about allowable residual drifts. McCormick *et al.* (2008) have proposed value of 0.5% as the allowable residual inter-story drift. They concluded that it is not economically justified to repair an earthquake-stricken building with residual inter-story drifts of more than 0.5%. While this conclusion was drawn according to Japanese practice, the same value can be expected for other countries as well. Meanwhile, some earlier studies (Sabelli *et al.* 2003, Kiggins and Uang 2006, and Erochko *et al.* 2011) have suggested that residual inter-story drifts of special moment resisting frames (SMRFs) can range from 0.3% to 1.2% under design-based earthquakes (DBE, 10% in 50 years). Accordingly, even well-proportioned MRFs are susceptible to excessive residual inter-story drifts.

In order to reduce residual deformations, different self-centering systems have been proposed earlier (Sheliang *et al.* 2004, Zhu and Zhang 2008, Tremblay *et al.* 2008, Kim and Christopoulos 2009, Zhou *et al.* 2014, Cheng and Chen 2014, and Salari and Asgarian 2015). It is shown that, among others, a backup elastic system can result in substantial reduction in residual deformations. Obviously, the secondary elastic system should have enough lateral stiffness to be able to push back the structure to its initial condition. Recent studies have also shown that nonlinear systems with high post-yield stiffness would experience lower residual deformations (Ruiz-Garcia and Miranda 2005, Mousavi and Zahrai 2016, and Baiguera *et al.* 2016).

As shown in Fig. 1, this study is intended to introduce a new Cable-Pulley Bracing (CPB) system by which wide MRFs with large openings can be braced. Note that it is difficult, if not impossible, to brace such frames with conventional braces. According to Fig. 1, the pre-tensioned cable elements connect two opposite corners of the frame using a bilinear path which turns around the opening(s). The bilinear configuration for the cable is provided by a pulley or sheave which is supported by a diagonal tension-only element, called “diagonal tie”. Further discussion and required formulations of the CPB system would be presented in the subsequent sections. It should be pointed out that a full circular pulley can also be used if the bracing cables are flexible enough. In this study, the term “cable” mainly refers to steel wire rope strands. However, other tension-only elements such as carbon fibers, glass fibers can also be used.

It should be pointed out that, current seismic codes (ASCE 7 2010, AISC 341 2005, Eurocode 8 2003 and ASCE 41 2006) have prohibited use of tension-only braces in regions with high seismicity

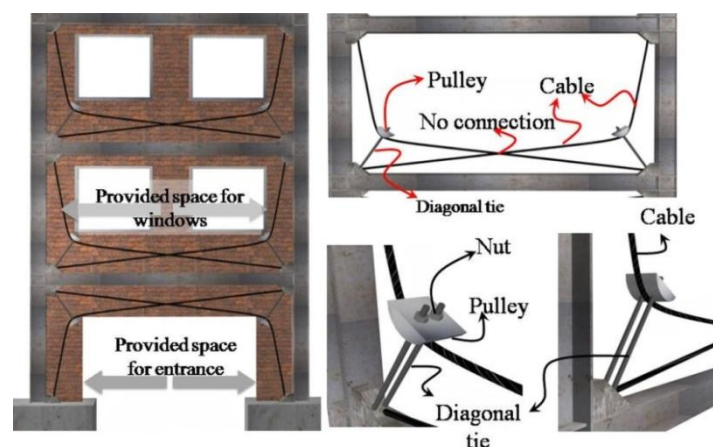


Fig. 1 Proposed cable-pulley bracing system

by imposing minimum values on slenderness of brace elements. While the reason is not explicitly mentioned, the authors believe that above policy stems from highly pinched hysteretic behavior of tension-only elements which would dramatically decrease energy dissipation capability of tension-only braces.

Regardless of the codes policy, some researchers (Pincheira 1992, Molaei and Saatcioglu 2013, Shalouf and Saatcioglu 2006, Welter 1991, Hou and Tagawa 2009, Mousavi and Zahrai 2016) have tried to investigate contribution of cable braces to seismically retrofit different steel and RC frames. Surprisingly, they obtained virtually the same results, that is, cable bracing can significantly improve lateral strength, initial stiffness, and post-yield stiffness of the frame. However, this technique failed to improve energy dissipation capability of the whole system due to the fact that cable elements are brittle. This brittleness can be easily explained from stress-strain curve of high strength strands. It is well understood that such materials suffer from small ultimate strains as well as lack of post-yield strain hardening. Both the former and the latter features make high strength strands, and consequently cable elements, quite brittle. As a result, the cable elements in the proposed CPB are intended to remain absolutely elastic. In the proposed bracing system, the cable elements have two main rules; first, to increase and optimally distribute lateral stiffness in different stories, and second, to act as an elastic backup system to decrease residual deformations. Meanwhile, seismic energies need to be dissipated through formation of plastic hinges in the frame itself. As a result, the proposed cable bracing system should be always combined with MRFs. In other words, the term ‘‘CPB’’ in this study refers to combination of cable-pulley braces and MRFs. Note that, the proposed technique is applicable for both seismic design of new buildings and seismic retrofit of existing structures.

## 2. Balanced pulley coordinate

A typical CPB is schematically depicted in Fig. 2. The rectilinear cable element, in fact, is composed of two linear cables with different orientations. Assuming a frictionless pulley, developed tensile forces in both cable parts would be the same. Note that the diagonal tie is a tension-only member and clearly in the balanced coordinate of the pulley, the imposed resultant force from the cable should be equal and coaxial with that imposed from the diagonal tie. Special care should be paid to inclination angle of the diagonal tie such that it can balance all imposed forces on the pulley. The authors would like to elaborate that this angle is not a practical concern, but need to be predefined during the design procedure of the CPB. Using static equilibrium equation, the balanced initial inclination of the diagonal tie can be obtained as follows

$$\left. \begin{aligned} \Sigma F_y = 0 \rightarrow T_d \sin \theta &= T_c (\sin \alpha_2 - \sin \alpha_1) \\ \Sigma F_x = 0 \rightarrow T_d \cos \theta &= T_c (\cos \alpha_1 - \cos \alpha_2) \end{aligned} \right\} \rightarrow \tan \theta = \frac{\sin \alpha_2 - \sin \alpha_1}{\cos \alpha_1 - \cos \alpha_2} \quad (1)$$

All parameters are defined in Fig. 2. Eq. (1) can be rewritten in terms of dimensional parameters as

$$\frac{h}{a} = \frac{\frac{H-h}{\sqrt{(H-h)^2 + a^2}} - \frac{h}{\sqrt{h^2 + (L-a)^2}}}{\frac{L-a}{\sqrt{h^2 + (L-a)^2}} - \frac{a}{\sqrt{(H-h)^2 + a^2}}} \quad (2)$$

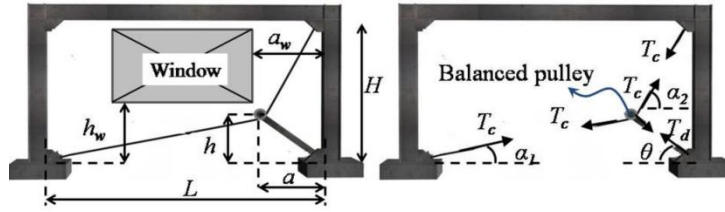


Fig. 2 Developed forces in the cable and pulley

Using some mathematics, Eq. (2) can be simplified to Eq. (3) which is an implicit equation with two unknown parameters. Parameters  $H$  and  $L$  have predefined values, according to the building architectural drawings, and parameters  $h$  and  $a$  are unknown

$$hL\sqrt{(H - h)^2 + a^2} - aH\sqrt{h^2 + (L - a)^2} = 0 \tag{3}$$

In order to solve Eq. (3), first a value should be assigned to one of the unknowns and then the equation can be solved for the other one. In any case, obtained/assumed values for the parameters  $a$  and  $h$  should satisfy the following inequalities

$$0 < a < a_w \quad , \quad 0 < h < h_w \tag{4}$$

Considering some frame heights and widths, required  $a$  and  $h$  are presented in Table 1.

Table 1 Balanced pulley coordinates and corresponding provided lateral stiffness. Elastic modulus of the cable assumed to be 100 GPa

$L$ (m)	$H$ (m)	$a$ (m)	$h$ (m)	$\alpha_1$ (°)	$\alpha_2$ (°)	$l_c$ (m)	$k_c$ (MN/m) $\Delta T < T_0$	$k_c$ (MN/m) $\Delta T \geq T_0$
6	3.5	0.4	0.42	4.3	82.6	8.72	$380A_c$	$190A_c$
		0.6	0.65	6.9	78.1	8.35	$1016A_c$	$508A_c$
		0.8	0.91	9.9	72.8	7.99	$2180A_c$	$1090A_c$
		1	1.19*	13.4	66.6	7.66	$4122A_c$	$2061A_c$
6	4	0.4	0.41	4.2	83.6	9.23	$266A_c$	$133A_c$
		0.6	0.64	6.8	79.9	8.85	$698A_c$	$349A_c$
		0.8	0.87	9.5	75.7	8.50	$1442A_c$	$721A_c$
		1	1.12*	12.6	70.9	8.17	$2633A_c$	$1316A_c$
8	3.5	0.4	0.43	3.2	82.6	10.71	$312A_c$	$156A_c$
		0.6	0.68	5.3	78.0	10.31	$840A_c$	$420A_c$
		0.8	0.95	7.5	72.6	9.93	$1804A_c$	$902A_c$
		1	1.28*	10.4	65.8	9.55	$3532A_c$	$1766A_c$
8	4	0.4	0.42	3.2	83.6	11.21	$220A_c$	$110A_c$
		0.6	0.66	5.1	79.8	10.82	$578A_c$	$289A_c$
		0.8	0.91	7.2	75.5	10.45	$1202A_c$	$601A_c$
		1	1.19*	9.6	70.4	10.08	$2230A_c$	$1115A_c$

\* Values more than 1 m for the parameter  $h$  might be impractical

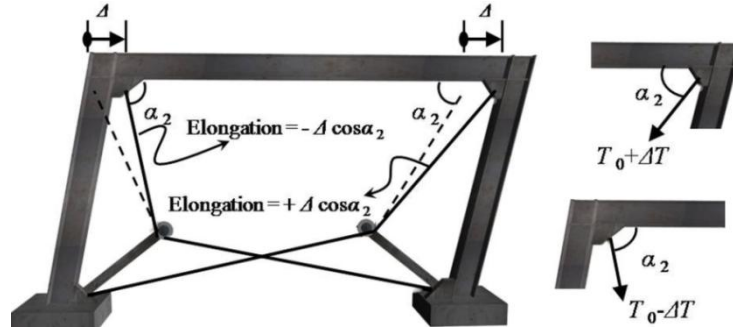


Fig. 3 Schematics of CPB under imposed lateral displacement

### 3. Lateral stiffness of the CPB

Consider a single span/single story CPB frame subjected to lateral interstory drift of  $\Delta$  as depicted in Fig. 3. Assuming pretension load of  $T_0$  for each cable, one of the cables tends to reduce its initial tensile force due to the imposed negative elongation and the other one tends to gain more tensile force responding to the imposed positive elongation.

The imposed negative/positive cable elongation,  $dl_c$ , can be simply estimated as

$$dl_c = \Delta \cos \alpha_2 \tag{5}$$

It should be pointed out that above elongation would be imposed on the full length of the cable, regardless of its rectilinear configuration. As a result, the corresponding change in the cable force can be evaluated as

$$\Delta T = E_c A_c d\varepsilon = \frac{E_c A_c \Delta \cos \alpha_2}{l_c} \tag{6}$$

In Eq. (6)  $\Delta T$  and  $d\varepsilon$  stand for the developed increment in the cable force and related axial strain, respectively. Besides, effective cross sectional area (net metallic area) of each cable is denoted by  $A_c$ .  $E_c$  is the elastic modulus of the cable element and full length of the cable (total of the both linear parts) is represented by  $l_c$ . According to the obtained change in the cable forces, lateral stiffness of the cable brace in the CPB can be evaluated as

$$k_c = \frac{((T_0 + \Delta T) - (T_0 - \Delta T)) \cos \alpha_2}{\Delta} \tag{7}$$

where  $k_c$  denotes lateral stiffness of the cable brace (including both bilinear cables). Obviously compressive strength of the cable element is zero and the cable with negative elongation cannot support any negative (compressive) force. As a result, two scenarios can be defined for the lateral stiffness of the cable braces in the CPB as formulated in Eq. (8).

$$k_c = \begin{cases} \frac{2E_c A_c \cos^2 \alpha_2}{l_c}, & \text{if } \Delta T < T_0 \\ \frac{E_c A_c \cos^2 \alpha_2}{l_c}, & \text{if } \Delta T \geq T_0 \end{cases} \tag{8}$$

In Eq. (8), the upper relation should be used when both rectilinear cables are in tension while the lower one should be used when one of the rectilinear cables loses its initial pre-tension load. Considering value of 100 GPa for the  $E_c$ , which is the case in most wire ropes, obtained lateral stiffnesses in various cases are also presented in Table 1. Combining Eqs. (6) and (8), a critical interstory drift,  $\Delta_{cr}$ , can be defined beyond which, lateral stiffness of cable braces in the CPB would be reduced by 50%.

$$\Delta_{cr} = \frac{T_0 l_c}{E_c A_c \cos \alpha_2} \quad (9)$$

Eq. (9) is a simple yet useful relation for choosing a suitable value for the cable pretension load,  $T_0$ . Note that, depending on the design philosophy, one needs to consider a tradeoff between  $T_0$  and  $\Delta_{cr}$ , as imposing a large sustained pretension load on the cable might be quite questionable, especially in the case of RC frames which can experience creep strains.

#### 4. Simplified FE model

Explicit modeling of the proposed CPB calls for defining a contact interaction between the cable and the pulley. This contact should allow separation and needs to be frictionless. While such rigorous techniques can be carried out by most general purpose FE packages, such as Abaqus (2011), with no doubt they are not suitable for professional engineers. As a result, in this section a simplified technique is proposed which is well suited for practical purposes.

In the mathematical model, the pulley can be replaced by a simple joint. This simplification leads to a triple-force joint in equilibrium, as illustrated in Fig. 4. It can be shown that in this configuration, the cable forces would still have the same values and such simplification has no effect on the developed diagonal tie force,  $T_d$ , i.e.,  $\lambda = \beta = 1$ .

Equilibrium equations at the joint give

$$\left. \begin{aligned} \Sigma F_y = 0 &\rightarrow \beta T_d \sin \theta = \lambda T_c \sin \alpha_2 - T_c \sin \alpha_1 \\ \Sigma F_x = 0 &\rightarrow \beta T_d \cos \theta = T_c \cos \alpha_1 - \lambda T_c \cos \alpha_2 \end{aligned} \right\} \rightarrow \tan \theta = \frac{\lambda \sin \alpha_2 - \sin \alpha_1}{\cos \alpha_1 - \lambda \cos \alpha_2} \quad (10)$$

Combining Eqs. (1) and (10), leads to

$$\frac{\sin \alpha_2 - \sin \alpha_1}{\cos \alpha_1 - \cos \alpha_2} = \frac{\lambda \sin \alpha_2 - \sin \alpha_1}{\cos \alpha_1 - \lambda \cos \alpha_2} \rightarrow \lambda = 1 \quad (11)$$

Accordingly in the simplified technique, the cable forces with different orientations are still the

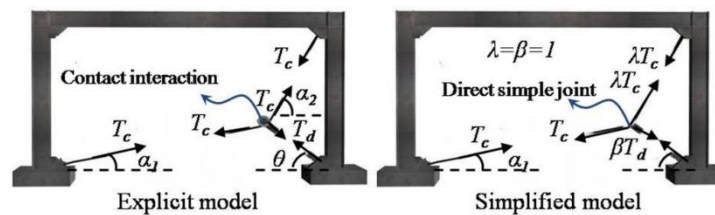


Fig. 4 Explicit and simplified numerical models

same. Consequently, it can be easily shown that  $\beta = 1$ , that is the proposed simplified technique would change neither stiffness nor strength of the cable-pulley brace. This claim is further examined in the subsequent section. It is crucial to note that the simplified technique is valid as far as the simple joint is placed exactly at the balanced coordinates of the pulley.

## 5. Numerical verification

As the proposed CPB is a mainly elastic system, its seismic behavior can be fully explained in terms of its lateral stiffness. In order to investigate accuracy of the proposed analytical and simplified FE model, three single story/single bay pinned steel frames are considered with height of 3.5 m and widths of 6 m, 8 m, and 10 m. The parameter  $a$  (see Fig. 2) is assumed to be 0.8 m in all cases and the parameter  $h$  would be obtained from Table 1, or Eq. (3). The cable element and the diagonal tie are assumed to have cross sectional area of 900 mm<sup>2</sup> and 1800 mm<sup>2</sup>, respectively, with zero pretension load. Note that analytical stiffness is obtained from Table 1 and the simplified model is built using SAP2000 (2010).

Moreover, Abaqus was used in the explicit modeling phase of the study. In the explicit modeling, shell and membrane elements are used for the pinned frame and the cable, respectively. The pulley is modeled with solid elements and a contact interaction is defined between the cable element and the pulley. Normal behavior of such used interaction allows separation and its transverse behavior is frictionless. Additionally, diagonal ties (not shown in Fig. 5) are modeled with two elastic axial springs. Obtained results are summarized in Table 2 and Fig. 5. It should be pointed out that presented stiffnesses would be doubled if substantial pretension load was previously developed in the cables.

Table 2 Comparison between different models in terms of lateral stiffness

Case	$L$ (m)	$H$ (m)	$a$ (m)	$h$ (m)	Analytical $k_c$ (MN/m)	Simplified $k_c$ (MN/m)	Explicit $k_c$ (MN/m)
1	6	3.5	0.8	0.91	1.96	1.95	1.97
2	8	3.5	0.8	0.95	1.62	1.57	1.65
3	10	3.5	0.8	0.98	1.39	1.39	1.43

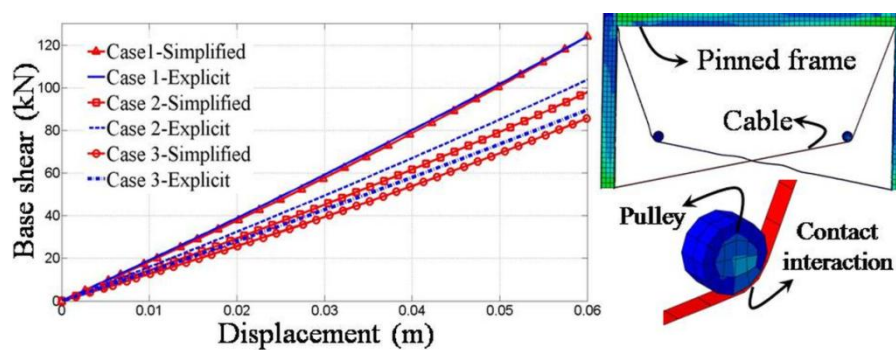


Fig. 5 Monotonic behavior of the cable-pulley braced frames

Table 3 Comparison between explicit and simplified models in terms of cable forces at different drifts  
(Cable forces are presented in kN)

Case	Drift = 0.5%		Drift = 1%		Drift = 1.5%	
	Simplified	Explicit	Simplified	Explicit	Simplified	Explicit
1	$T_{C1} = 96$	$T_{C1} = 113$	$T_{C1} = 218$	$T_{C1} = 230$	$T_{C1} = 331$	$T_{C1} = 352$
	$T_{C2} = 96$	$T_{C2} = 113$	$T_{C2} = 218$	$T_{C2} = 230$	$T_{C2} = 332$	$T_{C2} = 352$
2	$T_{C1} = 84$	$T_{C1} = 94$	$T_{C1} = 170$	$T_{C1} = 190$	$T_{C1} = 258$	$T_{C1} = 291$
	$T_{C2} = 84$	$T_{C2} = 94$	$T_{C2} = 170$	$T_{C2} = 190$	$T_{C2} = 258$	$T_{C2} = 291$
3	$T_{C1} = 73$	$T_{C1} = 80$	$T_{C1} = 151$	$T_{C1} = 162$	$T_{C1} = 232$	$T_{C1} = 248$
	$T_{C2} = 71$	$T_{C2} = 80$	$T_{C2} = 148$	$T_{C2} = 162$	$T_{C2} = 229$	$T_{C2} = 248$

Obtained results indicate that both analytical and simplified models are able to accurately estimate lateral stiffness of the cable braces. In order to further validate the proposed simplified model, developed cable forces at different inter-story drifts are presented in Table 3 in which  $T_{c1}$  and  $T_{c2}$  stand for the developed forces at the cables with  $\alpha_1$  and  $\alpha_2$  inclination angles, respectively.

## 6. Design procedure

In the CPB, the cable brace itself should be proportioned to remain in its elastic phase and on the other hand, MRF should be proportioned to dissipate substantial energy during strong seismic events. Accordingly, CPB differs from conventional dual lateral load resisting systems in which both systems should dissipate seismic energy through their nonlinear behavior.

While different conventional design procedures, such as  $m$ -factors and linear static analysis as recognized in ASCE 41 (2006), might be adopted for CPB, the authors proposed the following double-phase design procedure. The main intention of the proposed design philosophy is to obtain a rather linear pattern for the fundamental mode shape of the building. In this way, inter-story drifts of different stories would be virtually the same, at least in the first mode response.

### 6.1 Preliminary design

Preliminary design of the CPB is an iterative triple-step displacement-based procedure, as schematically shown in Fig. 6.

#### 6.1.1 MRF initial proportioning

MRFs need to be designed to carry different gravity load combinations and simultaneously proportioned per special moment resisting frame specifications. In other words, all beams and columns of the MRF need to be seismically compact and they should be proportioned according to the weak beam/strong column criteria. It is expected that such philosophy would provide sufficient lateral stiffness and strength for the MRFs to dissipate substantial energy during severe earthquakes. Accordingly, the used MRFs should be in compliance with specifications of the so called SMRFs as addressed in applicable codes of practice, such as AISC 341 (2005) or Eurocode 8 (2003).

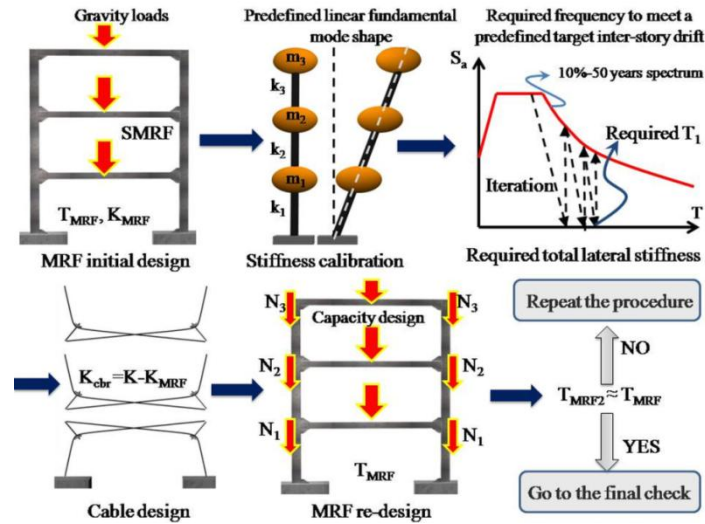


Fig. 6 Schematic procedure of the preliminary design for a sample 3-story CPB

6.1.2 Cable element design

The cables should be proportioned to result in a linear pattern for the first mode shape of the building. In this way, a rather uniform inter-story drift would be obtained along the height of the building. This can be done by using a well-documented procedure called, stiffness calibration. Detailed discussion about stiffness calibration is out of scope of the current study and can be found elsewhere (Connor 2003).

Considering a lumped mass shear building, the required distribution of the lateral stiffness along the height of the shear building would be as follows

$$K' = S^{-1}P' \tag{12}$$

where

$$\begin{cases} s(i, i) = \phi_i^* - \phi_{i-1}^* \\ s(i, i + 1) = \phi_i^* - \phi_{i+1}^* \\ s(i, j) = 0, \quad j \neq i, i + 1 \end{cases} \quad P' = M\Phi^* \tag{13}$$

In the above relations,  $K'$  is a vector defining the normalized lateral stiffness of each story,  $\Phi^*$  denotes the intended fundamental mode vector, and  $M$  represents mass matrix of the building. Assuming the same story height for all stories and a linear first mode pattern, according to Eq. (14), Eq. (13) can be simplified to Eq. (15)

$$\Phi^{*T} = \left\{ \frac{1}{n}, \frac{2}{n}, \dots, \frac{n}{n} \right\} \tag{14}$$

$$\begin{cases} s(i, i) = \frac{1}{n} \\ s(i, i + 1) = -\frac{1}{n} \\ s(i, j) = 0, \quad j \neq i, i + 1 \end{cases} \quad , \quad P'_i = \frac{i}{n} m_i \tag{15}$$

where,  $n$  and  $m_i$ , respectively, are number of stories and mass of the  $i$ th story. The required lateral stiffness at each story, to achieve  $\Phi^*$ , would be

$$K = \omega^2 K' \quad (16)$$

where  $\omega$  represents the first mode circular frequency of the building. Assuming an elastic design response spectrum,  $S_a(\omega, \zeta)$  and a target roof displacement for the first mode,  $q^*$ , one can obtain the required first mode frequency through an iterative procedure per Eq. (17)

$$\omega^2 = \frac{C_0 C_1 C_2 S_a(\omega, \zeta)}{q^*(1 - \zeta^2)} \quad (17)$$

In Eq. (17),  $\zeta$  is the damping ratio of the first mode and  $C_0$ ,  $C_1$ , and  $C_2$  are the modification factors as defined in ASCE 41 (2006).  $C_0$  is the first mode participation factor,  $C_1$  represents the ratio of inelastic displacement to its elastic counterpart and  $C_2$  accounts for cyclic behavior of the whole structure.

Note that CPB is not as stiff as conventional braced frames. Besides, the major lateral capacity of the CPB would be provided through elastic behavior of the cable elements which would neither degrade nor experience pinching. Accordingly, the parameters  $C_1$  and  $C_2$  can be considered to be 1, especially in the case of new designs in which the used MRFs would be well detailed. Clearly Eq. (17) is very similar to the relation of the target displacement as suggested in ASCE 41 (2006). However, one should bear in mind that the major part of the CPB would behave elastically making the effective period (or frequency) of the building virtually the same as its initial one. Validity of the aforementioned assumptions and simplifications would be verified in the subsequent section. Adopting a value of 5% for the first mode damping ratio of the building and a target maximum inter-story drift of  $\Delta_a$  for all stories, Eq. (17) can be simplified to

$$\omega^2 = \frac{C_0 S_a(\omega, \zeta)}{n \Delta_a} \quad (18)$$

where

$$C_0 = \frac{\sum_{i=1}^{i=n} \left(\frac{i}{n}\right) m_i}{\sum_{i=1}^{i=n} \left(\frac{i}{n}\right)^2 m_i} \quad (19)$$

For regular buildings with rather uniform mass distribution, value of  $C_0$  can be estimated according to the ASCE 41's approximate technique. Once the required first mode frequency of the building is obtained, the required lateral stiffness at each story can be evaluated using Eq. (16). Lateral stiffness of the cable braces at each story can be estimated as

$$k_{cbr\ i} = k_i - k_{MRF\ i} \quad (20)$$

in which  $k_i$ ,  $k_{cbr\ i}$ , and  $k_{MRF\ i}$  are total, cable brace, and MRF lateral stiffness at the  $i$ th story.  $k_{MRF\ i}$  can be estimated using Eqs. (12) and (16) if dynamic characteristics of the MRF alone were used, that is  $\Phi^*$  and  $\omega$  should be replaced by  $\Phi_{MRF}$  and  $\omega_{MRF}$ . According to Eq. (8) and assuming enough initial pretension load,  $T_0 > \Delta T$ , required net cross sectional area of the cable at the  $i$ th story and the  $j$ th bay can be estimated as

$$A_{c\ ij} = \frac{k_{cbr\ i} l_{c\ ij}}{2B_i E_c \cos^2 \alpha_{2\ ij}} \quad (21)$$

Note that  $B_i$  is the number of braced bays at the  $i$ th story and  $l_{cij}$  and  $\alpha_{2ij}$ , respectively, are the previously defined parameters  $l_c$  and  $\alpha_2$  at the  $i$ th story and the  $j$ th bay. As suggested earlier in Eq. (9), and substituting  $\Delta_{cr}$  with the allowable inter-story drift,  $\Delta_a$ , the required initial pretension load would be obtained according to Eq. (22).

$$T_{0\ ij} = \frac{E_c A_{c\ ij} \cos \alpha_{2\ ij}}{l_{c\ ij}} \Delta_a \quad (22)$$

It is expected that at the maximum inter-story drift, tensile force in the compression prone cable (with negative elongation) reduces to zero and the tensile force at the opposite cable increases to  $2T_0$ . Accordingly, ultimate strength of the cable material should be such that

$$\lambda^* T_{u\ ij} = \lambda^* A_{c\ ij} f_u > 2T_{0\ ij} \quad (23)$$

where  $f_u$  is the lower bound ultimate strength of the cable material and  $\lambda^*$  represents the required strength reduction factor. In the case of prestressed concrete design, many codes, such as ACI 318 (2008), have suggested a post-transfer force reduction factor of about 0.7. In contrast with prestressed concrete elements, however, cable elements in CPB have no frictional, shrinkage, creep, or even relaxation losses. Respect the fact that, as suggested by Collins and Mitchell (1987), relaxation loss would be a concern if the initial pretension load is selected to be more than 55%  $f_y$  (roughly 45%  $f_u$ ) which is not the case in CPB. According to ACI 318 (2008), developed stress in the cables should be limited to  $0.85f_u$  in the most extreme case (jacking). The most extreme condition that the CPB might face, is the maximum considered earthquake (MCE, 2%-50 years) as defined in ASCE 7 (2010) which can impose 50% higher elastic loads on the structure. Accordingly, appropriate reduction factor considering design level earthquake (10%-50 years) would be

$$\lambda^* = \frac{0.85}{1.5} = 0.55 < 0.7 \quad (24)$$

Therefore, acceptance criteria of the cable elements can be written as

$$0.55 A_{c\ ij} f_u > \frac{2E_c A_{c\ ij} \cos \alpha_{2\ ij}}{l_{c\ ij}} \Delta_a \rightarrow f_u > \frac{3.64 E_c \cos \alpha_{2\ ij}}{l_{c\ ij}} \Delta_a \quad (25)$$

If Eq. (25) fails to be satisfied, the maximum allowable inter-story drift needs to be decreased or a higher strength material should be used for the cable element. Developed forces in the diagonal ties are related to the cable forces through the following equation

$$T_d = \frac{\sin \alpha_2 - \sin \alpha_1}{\sin \theta} T \quad (26)$$

In typical cases,  $T_d$  ranges from  $0.7T$  to  $1.3T$ . Because diagonal ties commonly have higher cross sections compared to their corresponding cables, there is no concern about their acceptance criteria.

### 6.1.3 MRF re-check

Cable braces would induce additional axial demands on the columns and beams of the MRF. While cable loads have little effect on the beams due to contribution of the floor diaphragms, columns of the CPB should be checked and redesigned, if necessary, to carry vertical components of the cable force and the force exerted from the diagonal tie as well. Maximum expected value of the cable force is two times of its initial pre-tension load and the corresponding force at the diagonal tie can be estimated per Eq. (26). The aforementioned forces should be simultaneously placed on the beam/column joints of the CPB and the columns should be able to support this additional demand.

### 6.2 Final check

The final check (second phase of the design) is rather straightforward and calls for a nonlinear static or dynamic analysis. Acceptance criteria of beams, columns, connections, foundations, etc. are the same as those of conventional SMRFs, while cable elements as well as diagonal ties should remain elastic considering a significant resistance reduction factor as suggested in Eq. (24). Besides, all cables and diagonal ties, either with positive or negative elongations, should always remain in tension.

## 7. Numerical assessment

In order to evaluate contribution of the introduced CPB system and investigate the efficiency of the proposed design procedure, a typical 5-story residential building is considered, as illustrated in Fig. 7. The main focus of this section is on the E-W direction along which CPBs are placed on the exterior frames of the building. According to the architectural drawings, configuration of the

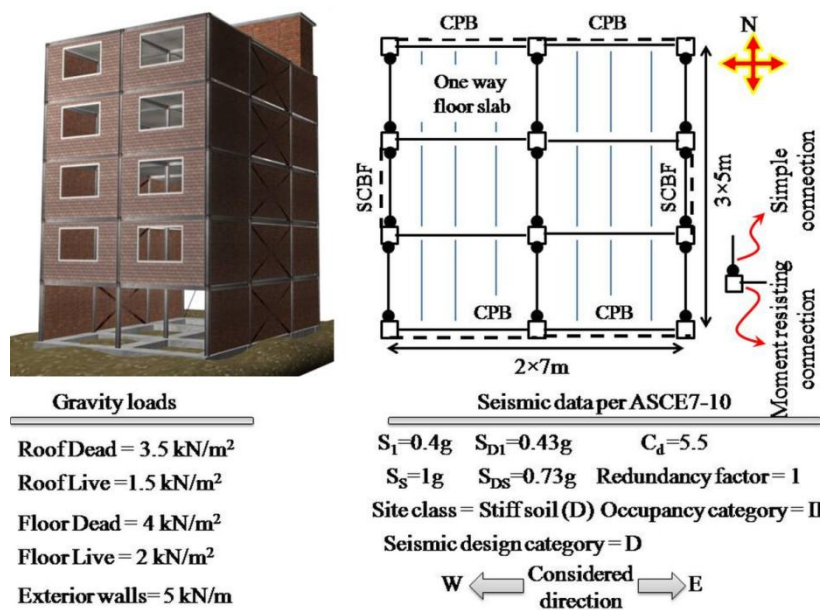


Fig. 7 Considered 5-story residential building

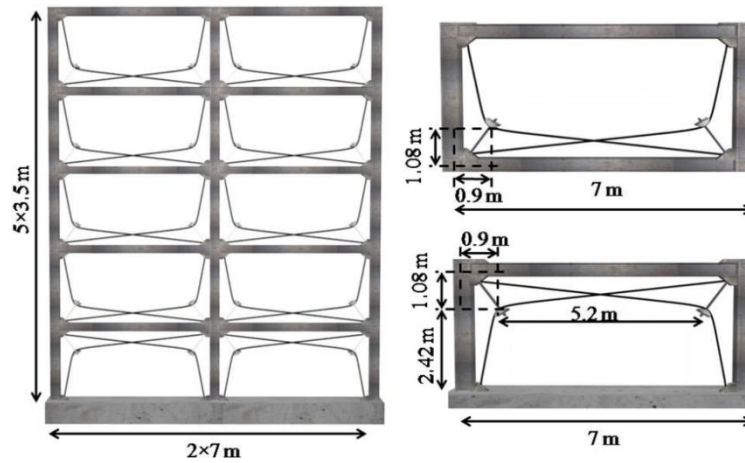


Fig. 8 Adopted configuration for the CPBs

Table 4 Dynamic characteristics of the designed MRF for gravity load combinations

Story	$M$ (ton)	$\phi_{MRF}$	$\omega_{MRF}$ (rad/s)	$P_{MRF}'$ (kN.s <sup>2</sup> /m)	$K_{MRF}'$ (MN.s <sup>2</sup> /m)	$K_{MRF}$ (MN/m)
1	126	0.193		24.30	1.9079	33.50
2	126	0.469		59.04	1.2461	21.88
3	126	0.714	4.19	89.89	1.1628	20.41
4	126	0.890		112.04	1.1079	19.45
5	83	1		82.95	0.7541	13.24

cable elements can be selected as those illustrated in Fig. 8. Note that the pulleys are placed on their balanced points according to Eq. (3) or equivalently Table 1. A36/ASTM steel with yield and ultimate stresses of 250 MPa and 375 MPa, respectively, and ultimate strain of 20% is used for the MRF while steel wire rope with ultimate strength of 1120 MPa and elastic modulus of 120 GPa is adopted as the cable and diagonal tie elements.

As the first step, the MRF is designed according to the gravity load combinations. Applicable codes of practice in this example are ASCE 7 (2010) and AISC 341 (2005). Obtained results are summarized in Table 4.

Again note that  $P'$ ,  $K'$ , and  $K$  for the MRF are obtained according to Eqs. (12) and (13) using  $\Phi_{MRF}$  instead of  $\Phi^*$ . The desired first mode vector is intended to be

$$\Phi^{*T} = \left\{ \frac{1}{5}, \frac{2}{5}, \frac{3}{5}, \frac{4}{5}, \frac{5}{5} \right\}$$

The maximum allowable inter-story drift is selected to be 1%. As a result, one can obtain  $\Delta_a = 0.01 \times 3.5 = 0.035$  m.

Using Eq. (19), participation factor of the first mode,  $C_0$ , would be 1.43 which is very close to the approximate value of 1.4 per ASCE 41. From Eq. (18), through an iterative procedure, the required fundamental period (frequency) of the building would be obtained as presented in Table 5. Note that  $S_a$  is obtained from ASCE 7-10's DBE (10%-50 years) spectrum

Table 5 Iterative procedure to obtain the required fundamental frequency

Iteration	$S_a$ (m/s <sup>2</sup> )	$\omega^2$ (rad <sup>2</sup> /s <sup>2</sup> )	Period (s)	Status
1	7.16	58.5	0.82	-
2	5.15	42.1	0.97	Not converged
3	4.35	35.6	1.05	Not converged
4	4.02	32.8	1.10	Not converged
5	3.87	31.6	1.12	Not converged
6	3.80	31.1	1.13	Not converged
7	3.73	30.5	1.14	Not converged
8	3.70	30.2	1.14	Converged

Table 6 Required total dynamic characteristics

Story	$M$ (ton)	$\phi^*$	$\omega$ (rad/s)	$P'$ (kN.s <sup>2</sup> /m)	$K'$ (MN.s <sup>2</sup> /m)	$K$ (MN/m)
1	126	0.2		25.18	1.67	50.62
2	126	0.4		50.36	1.55	46.81
3	126	0.6	5.50	75.54	1.30	39.19
4	126	0.8		100.71	0.92	27.77
5	83	1		82.95	0.41	12.54

The required dynamic characteristics of the whole structure, in E-W direction, are shown in Table 6. The last column of this table shows the required lateral stiffness of the building at each story. Simply using Eq. (20) by subtracting the last column of Table 4 from the last column of Table 6, required lateral cable stiffness can be estimated and consequently other cable parameters can be obtained as summarized in Table 7.

According to the adopted configuration for the cable braces, the following parameters in all stories and in all braced bays are fixed and known

$$B_i = 4, \quad \alpha_{2ij} = 69.6^\circ, \quad l_{cij} = 8.8 \text{ m}$$

Required cable parameters are reported in Table 7. Note that no cable brace is required at the top story.

Table 7 Design of cables for the CPB system

Story	$K_{cbr}$ (MN/m) Eq. (20)	$A_c$ in each bay (mm <sup>2</sup> ) Eq. (21)	$T_0$ at each cable (kN) Eq. (22)	Required strength Eq. (25)	$T_{d0}$ at each cable (kN) Eq. (26)	$A_d$ in each bay (mm <sup>2</sup> )
1	17.12	1290	215	Provided	215	1290
2	24.93	1875	310	Provided	310	1875
3	18.78	850	235	Provided	235	850
4	8.32	1415	105	Provided	105	1415
5	-0.7	-	-	-	-	-

Table 8 Maximum expected vertical cable forces on the columns of the CPB (upward forces have negative signs)

Story	$T_{cmax} = 2T_0$ (kN)	$T_{dmax} = 2T_{d0}$ (kN)	$N_{edge}$ (kN)	$N_{middle}$ (kN)
1	430	430	-400	-510
2	620	620	225	145
3	470	470	280	245
4	210	210	210	210
5	-	-	-	-

Table 9 First mode characteristics in two different structural systems

	Lateral load resisting system	T (s)	$\phi$ (fundamental mode shape)
Case I	CPB	1.14	{0.193, 0.426, 0.645, 0.843, 1}
Case II	SMRF	1.37	{0.147, 0.409, 0.671, 0.877, 1}

Now the already designed MRF should be re-checked for the maximum expected cable forces. Vertical components of cable and diagonal tie forces on each joint of the CPB should be evaluated at the maximum allowable inter-story drift as presented in Table 8. In this table,  $N_{edge}$  and  $N_{middle}$ , respectively, denote vertical components of the cable and diagonal tie forces on the edge and middle columns of the CPB.

The available column sections can easily carry these loads due to the fact that they are initially oversized according to strong column/weak beam specification. Therefore, there is no need to repeat the preliminary design procedure. To compare efficiency of the CPB to other structural systems, the adopted building is again designed per conventional SMRF specifications. Obtained fundamental period and mode shape of the building in each case are compared in Table 9. Obviously CPB could make the first mode inter-story drifts rather uniform without significantly changing period of the building. It is interesting to point out that obtained mode shape in the case of CPB is very close to the intended linear vector  $\phi^*$ .

As the second phase of the design, performance of the building is more evaluated through some nonlinear procedures. A 3D model of the building is created in the program SAP2000. Using the nonlinear behaviors specified in ASCE 41, lumped plastic hinges are assigned to the beams and columns. Inherent damping ratio of the building is 5% in all modes and P-delta effect is considered during all seismic analyses. Cable braces are also modeled with Cable Elements in SAP2000.

Two seismic hazard levels are considered per ASCE 7 that is Design Based Earthquake (DBE, 10%-50 years) and Maximum Considered Earthquake (MCE, 2%-50 years). Capacity curve of both structural systems, i.e., SMRF and CPB, including their maximum inter-story drifts are shown in Fig. 9. Adopted lateral force distribution in the nonlinear static procedure is based on the first mode vector of the structure. Note that SMRF was designed per AISC 341 and its required material (steel) weight is 440 kN, while this value in the case of CPB is 410 kN. As a result, the carried out comparison is quite fair. Overall results of the building are also represented in Table 10.

Note how a rather uniform inter-story drift distribution was achieved in the case of CPB. In the 2<sup>nd</sup> and 3<sup>rd</sup> stories, maximum drifts surpassed the maximum allowable value of 1% to some extent which can be attributed to the  $P$ - $\Delta$  effects as well as developed plastic hinges. It should be elaborated that reported performances of the building are evaluated using the ASCE 41's acceptance criteria.

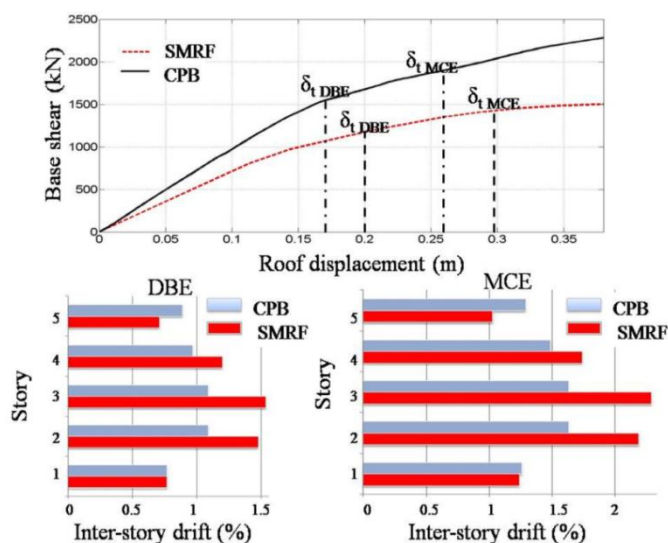


Fig. 9 Comparison between seismic behavior of SMRF and the proposed CPB

Table 10 Obtained results for the considered structural systems

Seismic hazard level	DBE		MCE	
	CPB	SMRF	CPB	SMRF
Target roof displacement, $\delta_r$ (m)	0.17	0.2	0.26	0.3
Maximum inter-story drift (%)	1.09	1.54	1.63	2.29
Shear capacity (kN)	1550	1170	1900	1430
Performance level	LS	LS	CP	CP

Table 11 Adopted mainshock-aftershock seismic records including 7 near-field and 7 far-field earthquakes

No.	Name	Station	$d$ (km)	Mag.	Un-scaled PGA (g)
1	Kocaeli	Izmit	4.8	7.4	0.220
2	Northridge	90056 Newhall	7.1	6.7	0.455
3	Chi Chi	WNT	1.18	7.6	0.626
4	Imperial Valley	5054 Bonds Corner	2.5	6.5	0.588
5	Tabas	Tabas	2.05	7.35	0.854
6	Chi Chi	TCU082	5.73	7.6	0.192
7	Parkfield	Cholame#5	5.3	6.1	0.442
8	Cape Mendocino	Rio Dell Overpass	18.5	7.1	0.549
9	Duzce	Lamont 1061	15.6	7.1	0.107
10	Northridge	Hollywood Store	25.5	6.7	0.358
11	Kobe	Nishi-Akashi	11.1	6.9	0.509
12	Imperial Valley	Delta	43.6	6.5	0.351
13	Landers	Yermo Fire Station	24.9	7.3	0.245
14	San Fernando	Lake Hughes#12	20.3	6.6	0.366

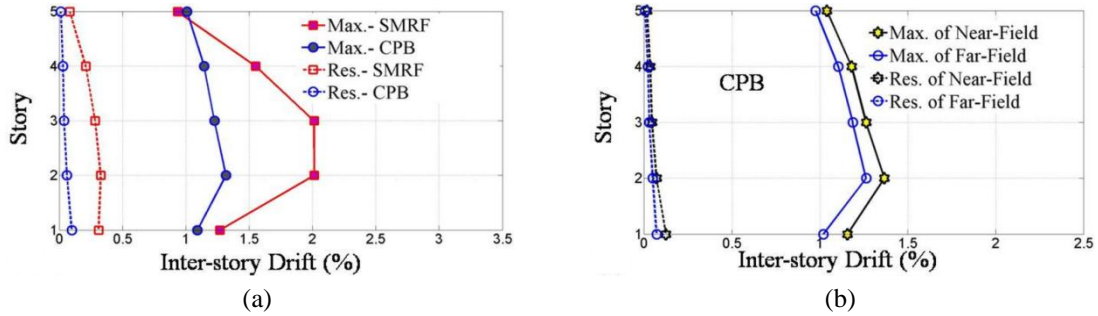


Fig. 10 (a) Maximum and residual inter-story drifts of the CPB and SMRF (average of 14 earthquakes); (b) Maximum and residual inter-story drifts of the CPB under Near-Field and Far-Field earthquakes

To evaluate contribution of the proposed CPB in terms of its self-centering capability, 14 mainshock-aftershock seismic sequences are considered. Considered ground accelerations are presented in Table 11. The mainshock records are scaled according to the spectrum-compatible scaling method as suggested in ASCE 7 while the aftershocks are obtained from the scaled mainshocks based on the proposed procedure by Das and Gupta (2010). It should be pointed out that a time gap of 20 s is considered between the mainshock and its aftershock.

Maximum and residual inter-story drifts are illustrated in Fig. 10. From Fig. 10(a) it can be observed that compared to SMRF, CPB would experience smaller maximum and residual inter-story drifts. Moreover, in the case of CPB, distribution of inter-story drifts is rather uniform which indicates contribution of all stories to the energy dissipation. In addition, maximum inter-story drifts of the CPB in all stories are close to the target value of 1%. According to the ASCE 7-10

Table 12 Obtained results for the considered CPB and SMRF under 14 earthquakes ( $V_{max}$  = maximum base shear,  $P_{cable-2}$  = developed axial force in one of the cable braces at the 2<sup>nd</sup> story)

	Mean ( $\mu$ )			Standard deviation ( $\sigma$ )		Dispersion index ( $\sigma^2/\mu$ )	
	CPB	SMRF	Difference	CPB	SMRF	CPB	SMRF
1 <sup>st</sup> drift-max (%)	1.1	1.3	-15%	0.15	0.27	0.02	0.06
2 <sup>nd</sup> drift-max (%)	1.3	2.0	-35%	0.11	0.29	0.01	0.04
3 <sup>rd</sup> drift-max (%)	1.2	2.0	-40%	0.11	0.23	0.01	0.03
4 <sup>th</sup> drift-max (%)	1.1	1.6	-31%	0.10	0.19	0.01	0.02
5 <sup>th</sup> drift-max (%)	1.0	0.9	+11%	0.10	0.10	0.01	0.01
1 <sup>st</sup> drift-res (%)	0.10	0.31	-68%	0.06	0.31	0.03	0.31
2 <sup>nd</sup> drift-res (%)	0.06	0.33	-82%	0.04	0.29	0.02	0.25
3 <sup>rd</sup> drift-res (%)	0.04	0.28	-86%	0.03	0.23	0.02	0.19
4 <sup>th</sup> drift-res (%)	0.03	0.21	-86%	0.02	0.12	0.02	0.07
5 <sup>th</sup> drift-res (%)	0.01	0.08	-88%	0.02	0.04	0.02	0.02
$d_{roof-max}$ (mm)	188	256	-27%	13.29	29.02	0.94	3.29
$d_{roof-res}$ (mm)	6	41	-85%	4.23	33.57	2.80	27.23
$V_{max}$ (kN)	2027	1754	+16%	1.39	4.15	0.00	0.01
$P_{cable-2}$ (kN)	612	-	-	4.31	-	0.01	-

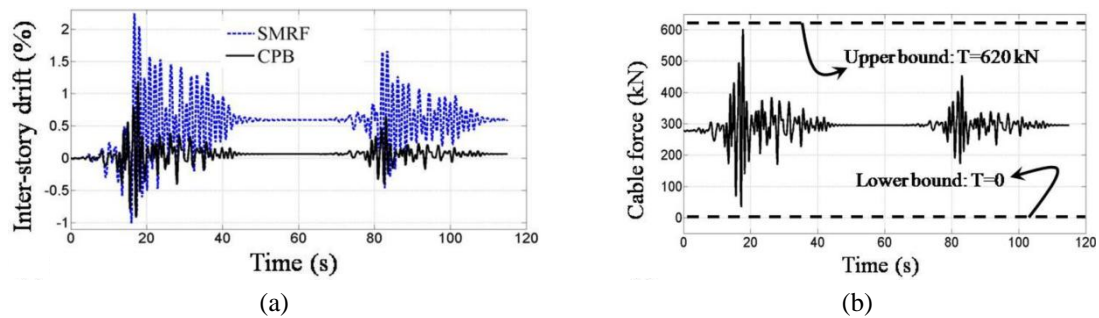


Fig. 11 (a) Inter-story drift of the 2<sup>nd</sup> story; and (b) cable force at the 2<sup>nd</sup> story under Earthquake #13

allowable inter-story drift can be increased by 25% as time-history analyses are carried out. Accordingly, the allowable inter-story drift of the considered CPB would be 1.25%. Fig. 10(a) indicates that inter-story drifts of the CPB in all stories are less than 1.25%. In order to evaluate behavior of the CPB separately under the Near-Field and Far-Field earthquakes, obtained results are averaged separately for Near- and Far-Field earthquakes. Fig. 10(b) shows that Near-Field earthquakes generally would result in higher demands, as expected.

Values of the maximum inter-story drifts, roof displacement, base shear, and axial force of the 2<sup>nd</sup> story cable brace are presented in Table 12. CPB can reduce maximum inter-story drifts up to 40% at the expense of 16% increase in the base shear. Moreover, maximum and residual roof displacements are reduced by 27% and 85%, respectively, in the case of CPB. Comparing standard deviation and dispersion index of the obtained responses, it can be concluded that behavior of the CPB is less dispersed under different earthquakes. Also note that the maximum cable force at the 2<sup>nd</sup> story of the CPB is 612 kN which is close to the intended value of  $T_{cmax} = 620$  kN under DBE seismic hazard (see Table 8). In order to present further details about the obtained results, time histories of the 2<sup>nd</sup> story drift and the developed axial force in the 2<sup>nd</sup> story cable brace, under the Earthquake #13 are shown in Fig. 11.

## 8. Conclusions

A Cable-Pulley Brace (CPB) system is introduced which is well suited for wide frames with large openings, either windows or entrances. Required analytical and numerical models of the CPB are derived and verified by different techniques. CPB includes a gravity-based designed MRF, braced with cable elements with rectilinear configurations. While the required energy dissipation would be provided by the MRF, the cable braces would increase lateral stiffness and significantly improve self-centering capability of the whole system. Using a simplified FE model, the CPB can be analyzed by conventional engineering computer software, making the system well suited for practical applications.

A simple but efficient enough design procedure is investigated for the CPB. The proposed displacement-based design philosophy would lead to a rather uniform inter-story drift distribution along the height of the building with a predefined value for the allowable inter-story drift. Considering a 5-story building, efficiency of the proposed design procedure was investigated and seismic behavior of the CPB was compared to that of a conventional SMRF. According to the obtained results, compared to SMRF, CPB has lower maximum and residual inter-story drifts.

Besides, CPB would not impose additional constructional costs on the project. For example, required steel weight for the designed 5-story SMRF is about 440 kN while this value in the case of CPB is only 410 kN still resulting in significant improvements in the seismic behavior of the building with no interruption for the probable required openings.

Finally, the authors would like to point out that the proposed CPB is an ongoing technology and this is just primary research to investigate its contribution. To thoroughly explore different features of the proposed CPB, further analytical, numerical, and experimental studies are still required.

## References

- Abaqus (2011), V 6.11, DassaultSystemesSimulia Corp.; Providence, RI, USA.
- ACI 318 (2008), Building code requirements for structural concrete, American Concrete Institute; MI, USA.
- AISC 341 (2005), Seismic provisions for structural steel buildings, American Institute of steel construction Inc.; Chicago, IL, USA.
- ASCE 7 (2010), Minimum Design Loads for Buildings and Other Structures, American Society American Society of Civil; Reston, VA, USA.
- ASCE 41 (2006), Seismic rehabilitation of existing buildings, American Society of Civil Engineers; Reston, VA, USA.
- Baiguera, M., Vasdravellis, G. and Karavasilis, T.L. (2016), "Dual seismic-resistant steel frame with high post-yield stiffness braces for residual drift reduction: Numerical evaluation", *J. Construct. Steel Res.*, **122**, 198-212.
- Cheng, C.T. and Chen, F.L. (2014), "Seismic performance of a rocking bridge pier substructure with frictional hinge dampers", *Smart Struct. Syst., Int. J.*, **14**(4), 501-516.
- Collins, M.P. and Mitchell, D. (1987), *Prestressed Concrete Basics*, Canadian Prestressed Concrete Institute (CPCI), Ottawa, ON, Canada.
- Connor, J.J. (2003), *Introduction to Structural Motion Control*, Prentice Hall, Upper Saddle River, NJ, USA.
- Das, S. and Gupta, V.K. (2010), "Scaling of response spectrum and duration for aftershocks", *Soil Dyn. Earthq. Eng.*, **30**(8), 724-735.
- Erochko, J., Christopoulos, C., Tremblay, R. and Choi, H. (2011), "Residual drift response of SMRFs and BRB frames in steel buildings designed according to ASCE 7-05", *J. Struct. Eng.*, **137**(5), 589-599.
- Eurocode 8 (2003), Design of structures for earthquake resistance- Part 1: General rules, seismic actions and rules for buildings, European Committee for Standardization, Brussels, Belgium.
- Hou, X. and Tagawa, H. (2009), "Displacement-restraint bracing for seismic retrofit of steel moment frames", *J. Construct. Steel Res.*, **65**(5), 1096-1104.
- Kiggins, S. and Uang, C.M. (2006), "Reducing residual drift of buckling restrained braced frames as a dual system", *Eng. Struct.*, **28**(11), 1525-1532.
- Kim, H.J. and Christopoulos, C. (2009), "Numerical models and ductile ultimate deformation response of post-tensioned self-centering moment connections", *Earthq. Eng. Struct. Dyn.*, **38**(1), 1-21.
- McCormick, J., Aburano, H., Ikenaga, M. and Nakashima, M. (2008), "Permissible residual deformation levels for building structures considering both safety and human elements", *Proceedings of the 14<sup>th</sup> World Conference on Earthquake Engineering*, Beijing, China, October.
- Molaei, A. and Saatcioglu, M. (2013), "Seismic retrofit of reinforced concrete frames with diagonal prestressing cables", Research Report; Ottawa-Carleton Earthquake Engineering Research Center, OT, Canada.
- Mousavi, S.A. and Zahrai, S.M. (2016), "Contribution of pre-slacked cable braces to dynamic stability of non-ductile frames; An analytical study", *Eng. Struct.*, **117**, 305-320.
- Pincheira, J.A. (1992), "Seismic strengthening of reinforced concrete frames using post-tensioned bracing systems", Ph.D. Dissertation; The University of Texas at Austin, TX, USA.
- Ruiz-Garcia, J. and Miranda, E. (2005), "Performance-based assessment of existing structures accounting

- for residual displacements”, John A. Blume Earthquake Engineering Center, Report No. 153; Stanford University, CA, USA.
- Sabelli, R., Mahin, S. and Chang, C. (2003), “Seismic demands on steel braced frame buildings with buckle restrained braces”, *Eng. Struct.*, **25**(5), 655-666.
- Salari, N. and Asgarian, B. (2015), “Seismic response of steel braced frames equipped with shape memory alloy-based hybrid devices”, *Struct. Eng. Mech., Int. J.*, **53**(5), 1031-1049.
- SAP 2000 (2010), Version 14.2.2, Computers and Structures, Inc., CA, USA.
- Shalouf, F. and Saatcioglu, M. (2006), “Seismic retrofit of non-ductile reinforced concrete frames with diagonal prestressing”, *Proceedings of the 8th U.S. National Conference on Earthquake Engineering*, San Francisco, CA, USA, April.
- Sheliang, W., Xindong, Z., Wang, S. and Junqiang, Z. (2004), “The seismic response analysis of isolation structure with shape memory alloy recentering dampers”, *Proceedings of the 10<sup>th</sup> JSSI Symposium On Performance of Response Controlled Buildings*, Yokohama, Japan, November, Paper No. 111.
- Tremblay, R., Lacerte, M. and Christopoulos, C. (2008), “Seismic response of multistory buildings with self-centering energy dissipative steel braces”, *J. Struct. Eng.*, **134**(1), 108-120.
- Welter, J.E. (1991), “Retrofit strengthening of a seismically inadequate reinforced concrete frame using prestressed cable bracing systems and beam alteration”, M.Sc. Thesis; The University of Oklahoma, OK, USA.
- Zhou, Z., He, X.T., Wu, J., Wang, C.L. and Meng, S.P. (2014), “Development of a novel self-centering buckling-restrained brace with BFRP composite tendons”, *Steel Compos. Struct., Int. J.*, **16**(5), 491-506.
- Zhu, S. and Zhang, Y. (2008), “Seismic analysis of concentrically braced frame systems with self-centering friction damping braces”, *J. Struct. Eng.*, **134**(1), 121-131.

BU